Supplemental Figures

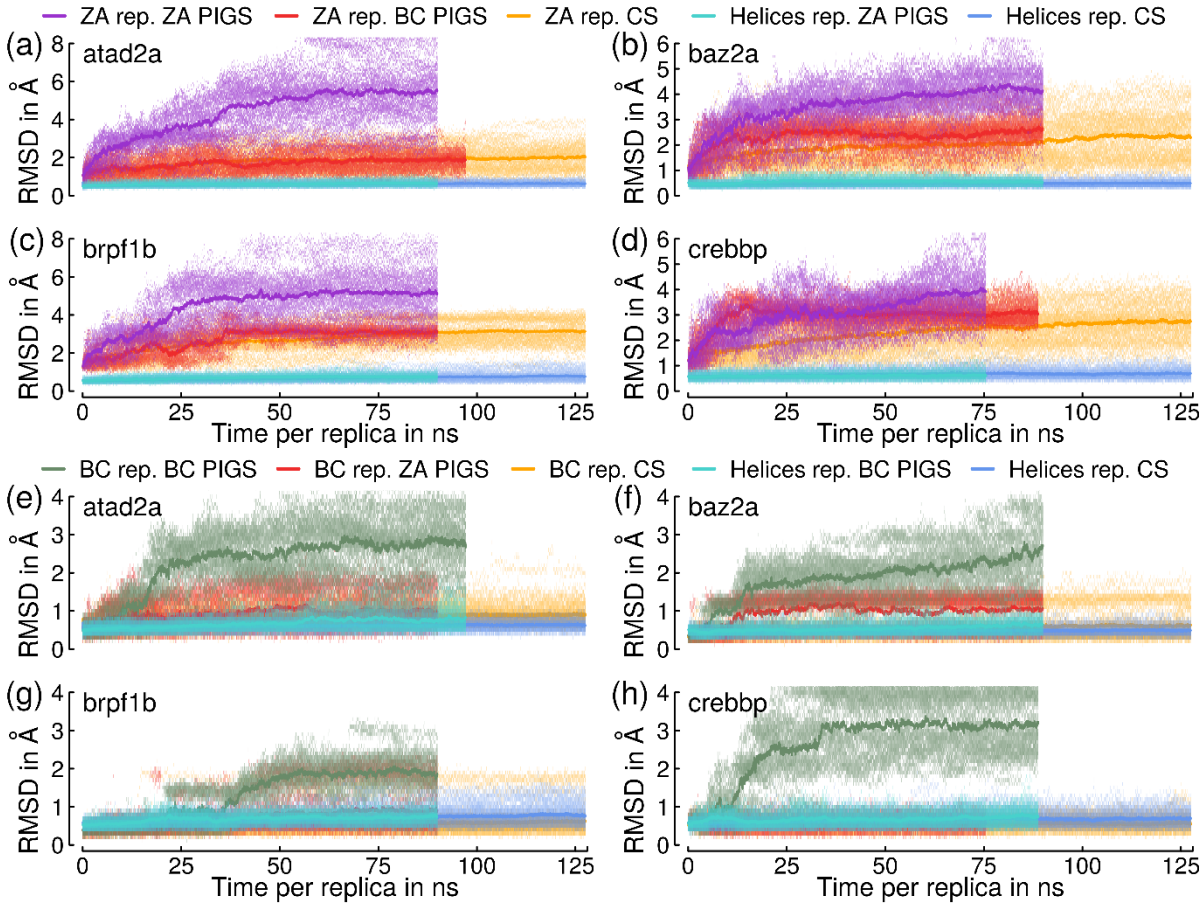

Figure S1. Root mean square deviation traces when not using Markov state model (MSM) steady state weights (see 2.6). This figure is identical to Figure 2 in the main text except that the raw sampling weights (counts) were used to compute the averages and accumulate the 2D histograms (envelopes). See the caption to Figure 2 and Section 2.3 in the main text for details.

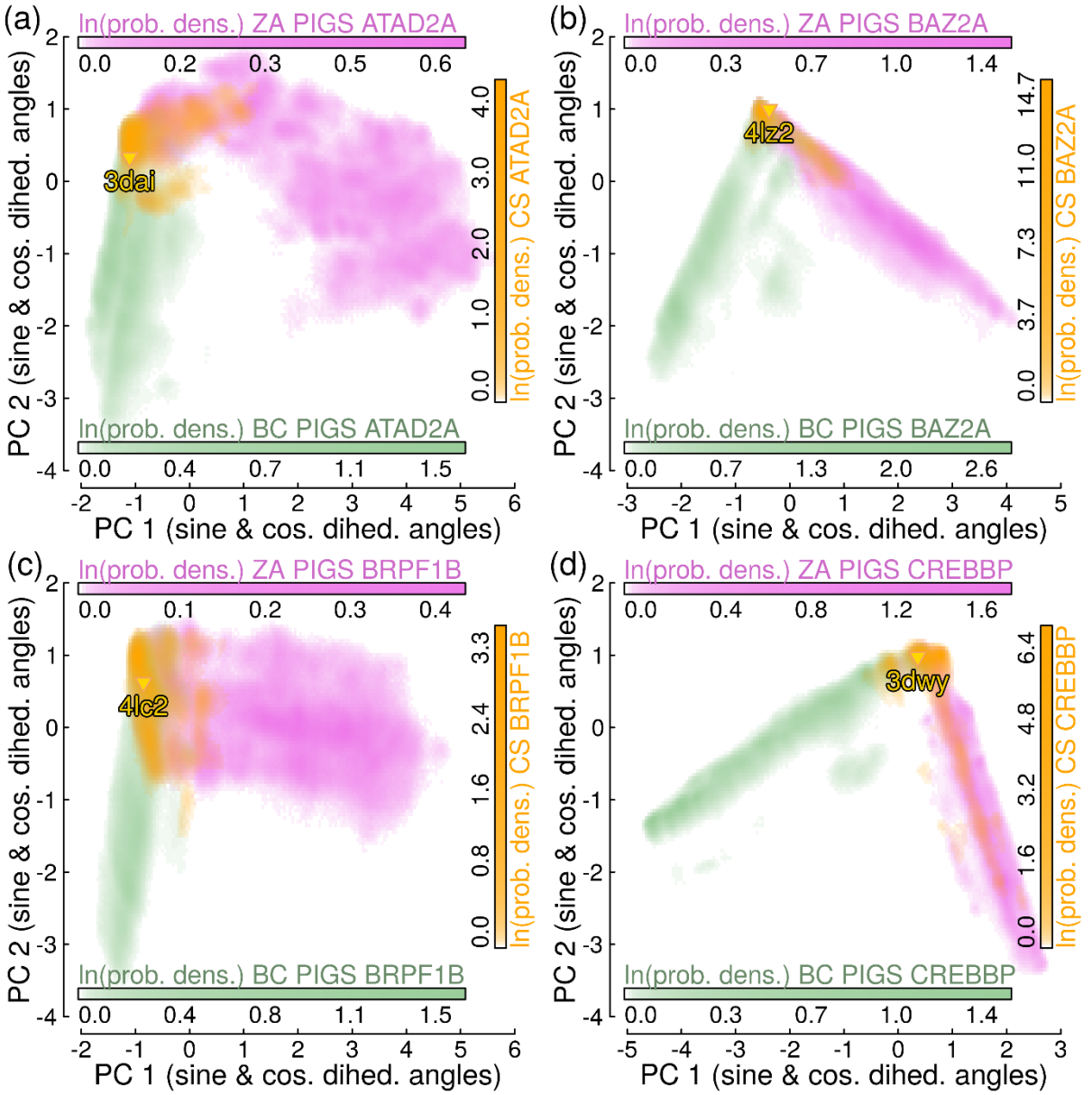

Figure S2. Principal component (PC) projections when not using MSM steady state weights (see 2.6). This figure is identical to Figure 3 in the main text except that the raw sampling weights (counts) were used to accumulate the 2D histograms. See the caption to Figure 3 and Section 2.4 in the main text for details.

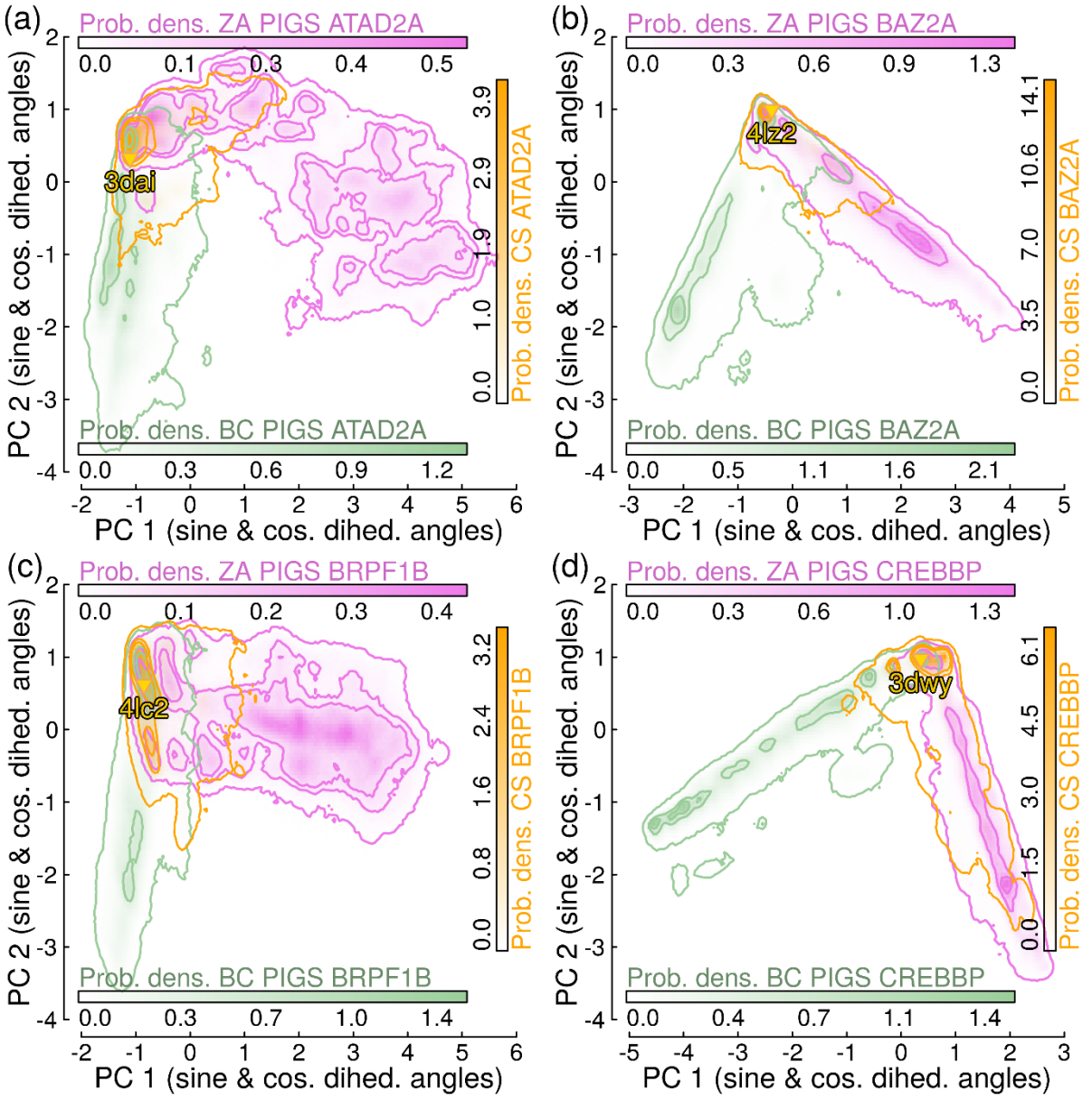

Figure S3. Principal component (PC) projections when plotted in linear scale. This figure is identical to Figure 3 in the main text except that the 2D histograms are plotted in a linear transparency scale and that three contour lines per simulation group are added per panel. See the caption to Figure 3 and Section 2.4 in the main text for details. For a given simulation group histogram, the contour lines are computed as follows. The minima and maxima across nonzero bins are rounded up and down to the nearest multiple of 10, respectively. The lower value is multiplied by 5, and the 3 contour levels correspond to this lower value, the larger value, and their mean.

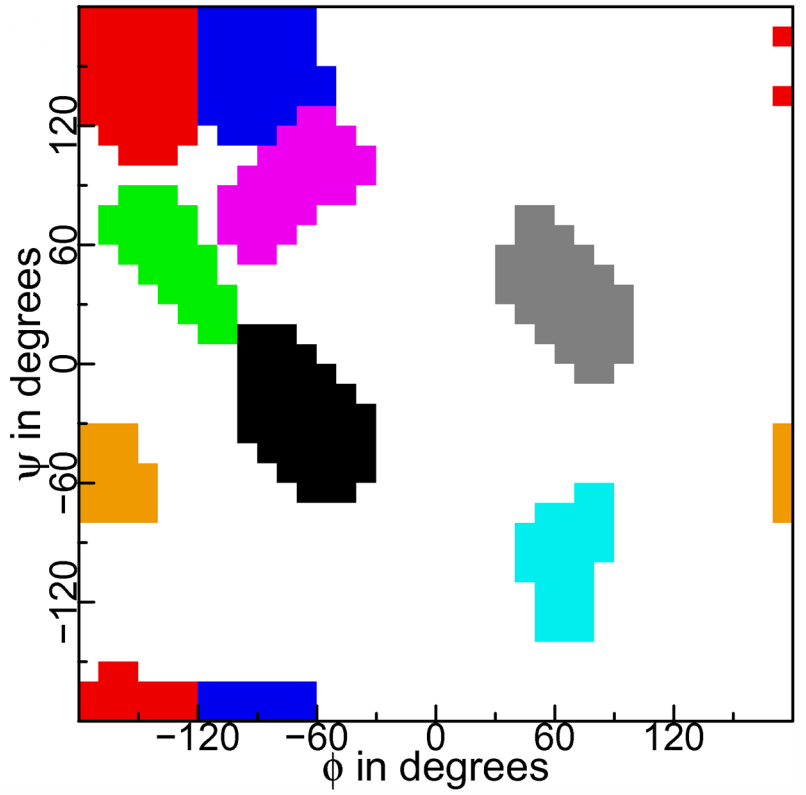

Figure S4. Coarse states in Ramachandran space. For each residue in the respective bromodomains, ϕ and ψ angles are used to assign its torsional state according to 8 predefined regions of the Ramachandran map, *e.g.*, the α-helical basin, which is in black. Areas in white correspond to forbidden or very low likelihood regions. For the count of discovered states for every stretch of 3 consecutive residues (used in Figure 4 in the main text), we mandated that all 3 three residues dwell in one of the 8 colored regions. Otherwise, the state was not counted. No special treatment was applied for glycine in order to not have additional states in a stretch-specific manner. The lack of states in the lower right-hand side of the map means that counts for stretches involving glycine may be underestimated. However, there is no glycine residue in the BC loops of any of the 4 domains (see Figure 1a in the main text). There is a single glycine residue in the ZA loops of brpf1b, crebbp, and baz2a, and none in the ZA loop of atad2a. Overall there are 1, 4, 3, and 5 glycine residues in atad2a, brpf1b, crebbp, and baz2a, respectively.

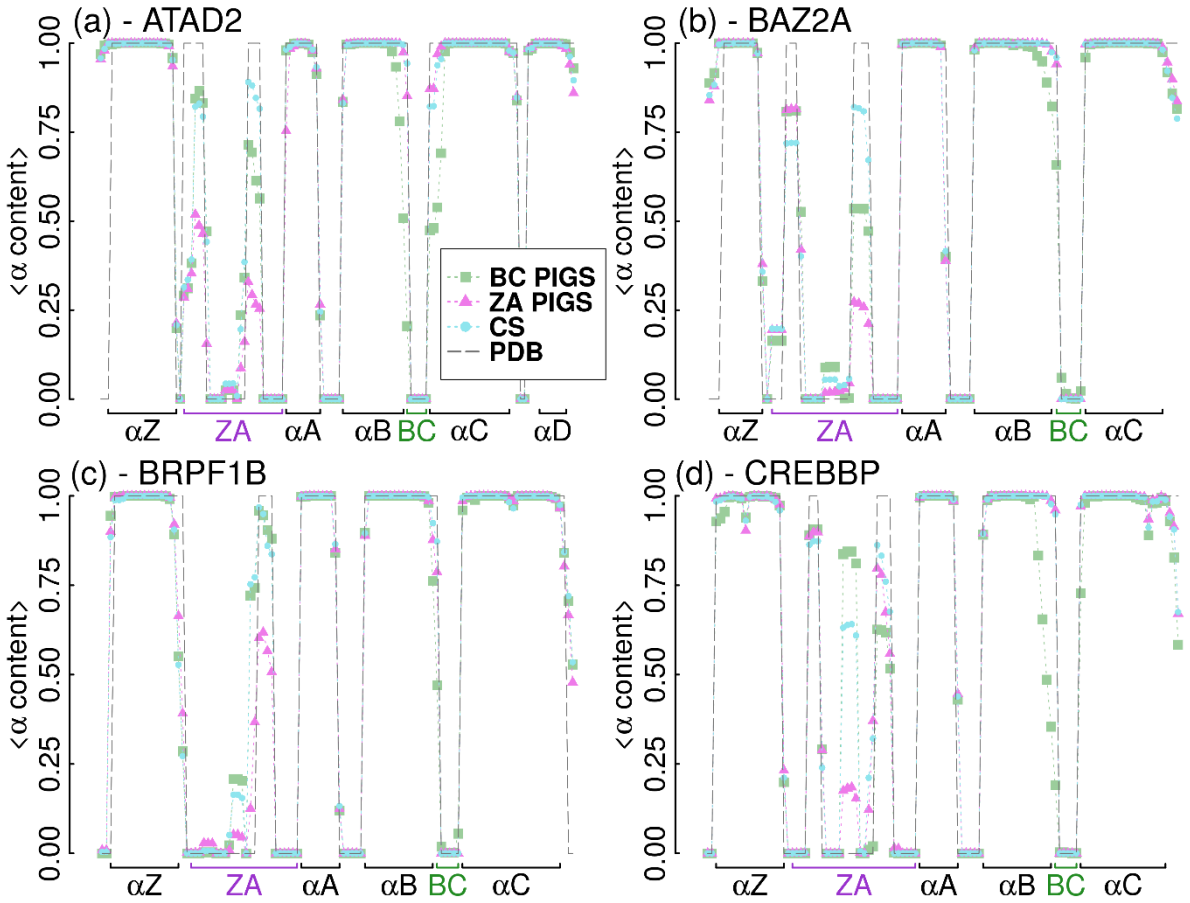

Figure S5. The average α-helical content per residue when not using MSM steady state weights (see 2.6). This figure is analogous to Figure 4 in the main text except that the raw sampling weights (counts) were used to calculate the average α-helical contents. The counts for discovered states are omitted here since they do not depend on MSM weights. See the caption to Figure 4 in the main text for details.

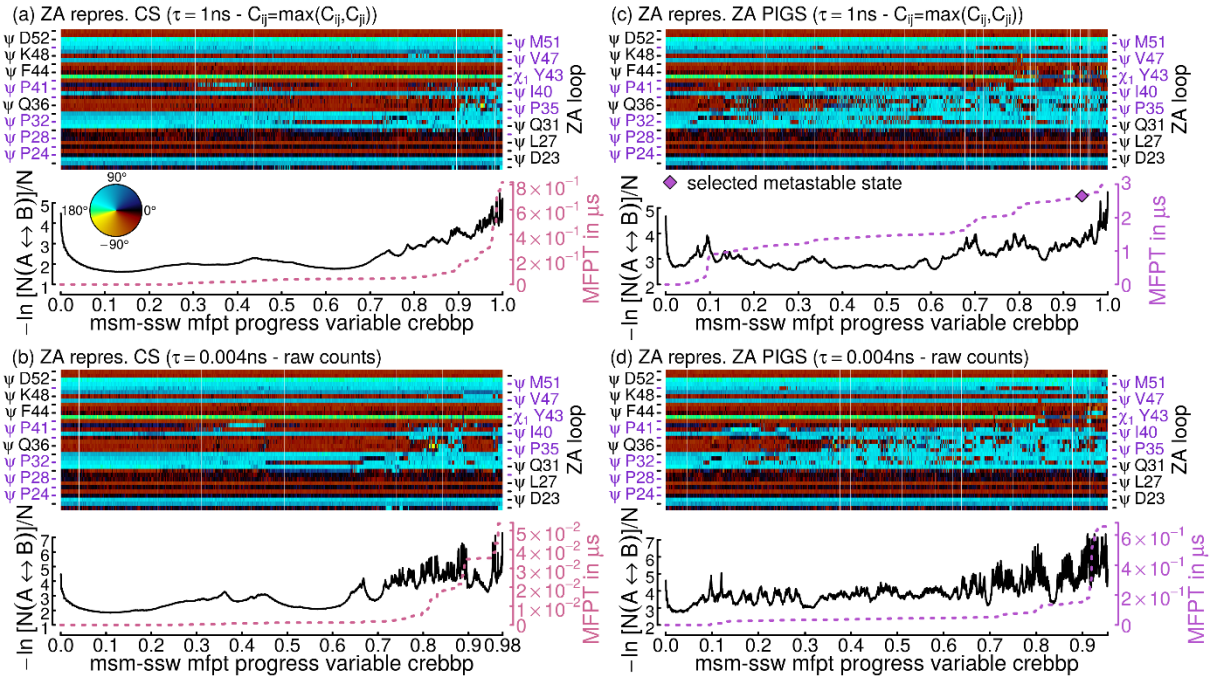

Figure S6. Mean first passage times (MFPTs) for the ZA loop in crebbp in the CS and ZA PIGS simulation groups. In analogy to Figure 6 in the main text, we plot ZA loop MFPTs, cut-profiles, and torsional state annotations for the crebbp bromodomain in CS and ZA PIGS. The MFTPs plotted in panels (a) and (c) are the same ones drawn in Figure 5d in the main text for CS and ZA PIGS, respectively. MFPTs are also used to order the states along the x-axis, which are spaced by their steady state weights (derived from the individual networks as explained in 2.5). Cut profiles (black lines) report on the barriers between the states on the left and the states on the right at a given point. Torsional annotations are at the top, and the axis labels are found both left and right to improve legibility. The angles included in the ZA PIGS representation (Table I in the main text) are highlighted in purple font. For each angle, the value of the centroid of each cluster is taken as a consensus value (vertical white lines are due to resolution limitations of raster images). The color wheel in (a) for the torsion angle values applies to all panels. **(a)** CS, τ = 1.0ns and detailed balance is imposed with naïve symmetrization of the count matrix (see 2.5 in the main text). **(b)** CS, τ = 0.04ns and detailed balance is not imposed. **(c)** Same as (a) for ZA PIGS. **(d)** Same as (b) for ZA PIGS.

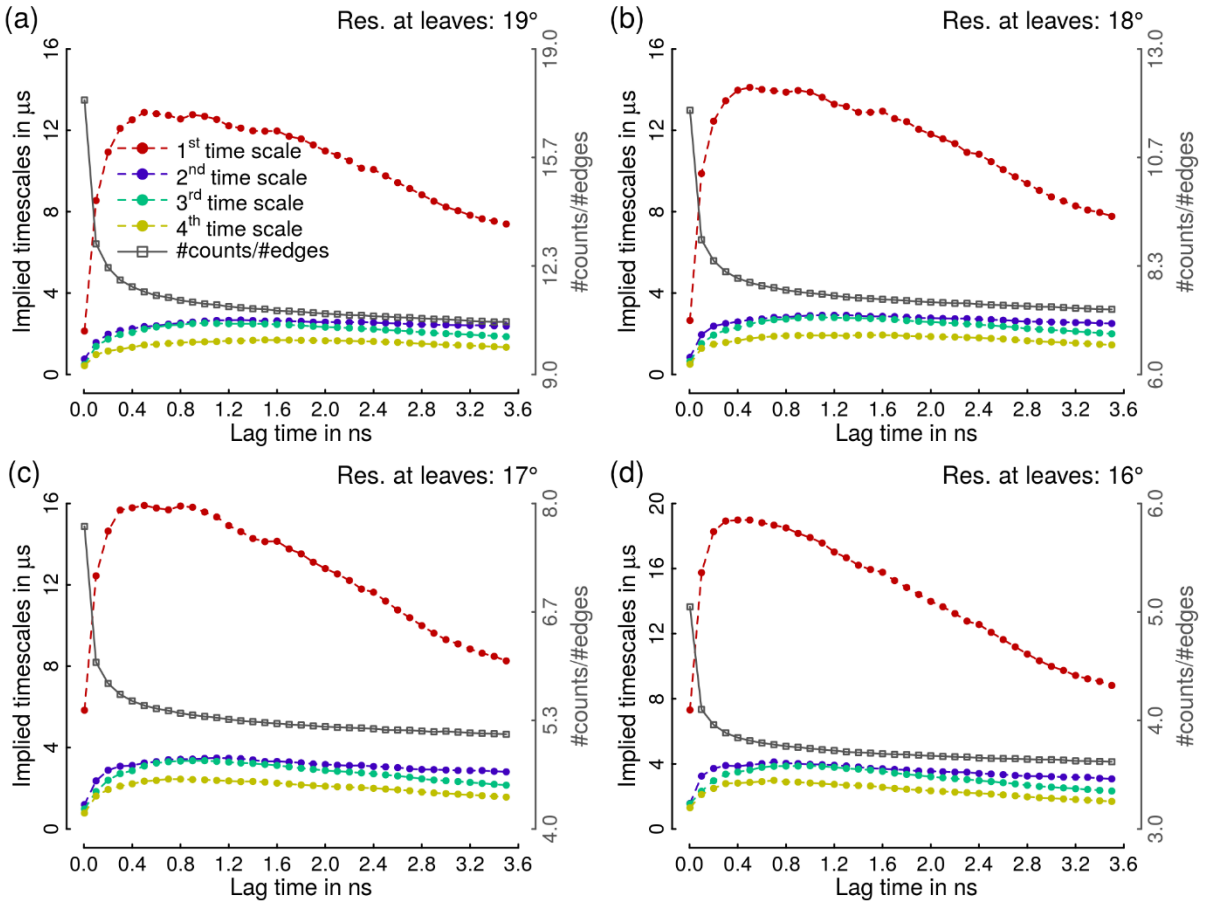

Figure S7. Implied time scales as a function of lag time and clustering resolution for atad2a. The slowest four implied time scales calculated from the 2nd to 5th largest eigenvalues are plotted along with the average number of transition counts per edge. Data are plotted as a function of lag time and for different clustering resolutions (snapshots from all simulation groups are used jointly, see 2.6 in the main text). We included all the degrees of freedom listed in Table III of the main text in a joint representation for grouping snapshots into clusters. Detailed balance is imposed by naïve symmetrization of the count matrix. The legend in panel (a) applies to all panels. **(a)-(d)** Data for target clustering resolutions of 19°, 18°, 17°, and 16°, respectively. The number of counts per network edge decreases with increasing lag time and finer resolution as expected, yet the behavior of the time scales is quite robust. The analogous plots below (Figures S8-S10) exhibit similar trends, and we settled on a resolution of 17° and a lag time of 1.0 ns, which appears to be a reasonable choice for all but the slowest mode for baz2a (Figure S10).

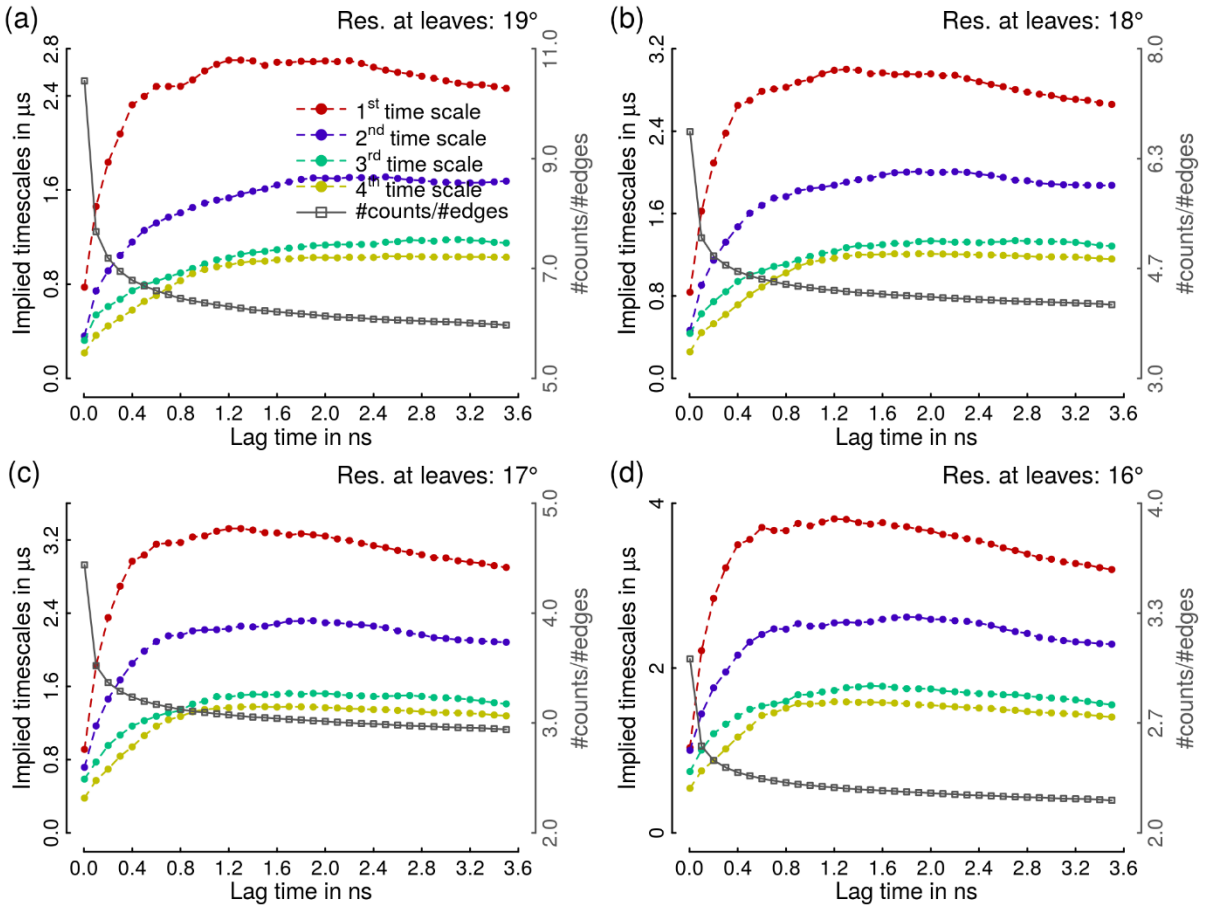

Figure S8. Implied time scales as a function of lag time and clustering resolution for brpf1b. This figure is identical to Figure S7 except that data for the bromodomain of brpf1b are shown.

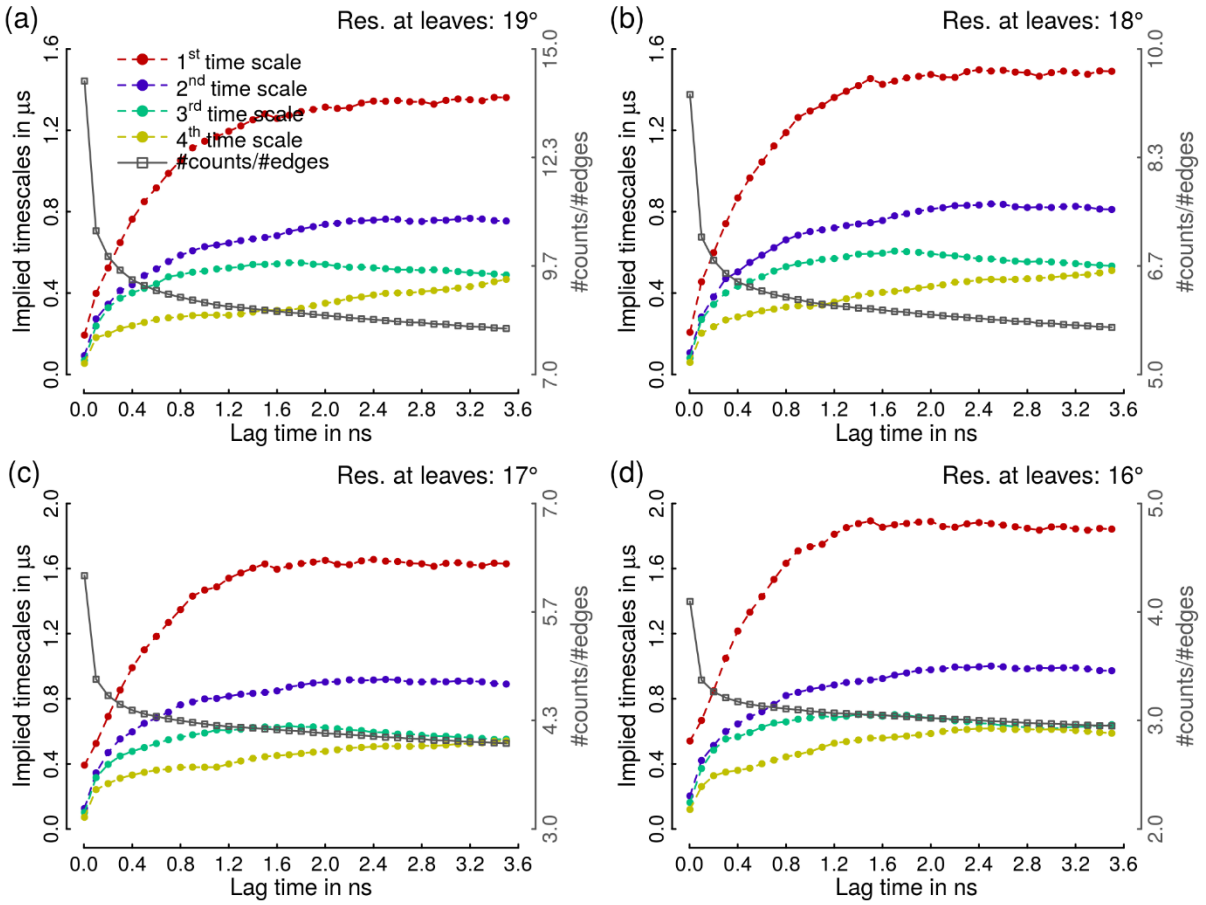

Figure S9. Implied time scales as a function of lag time and clustering resolution for crebbp. This figure is identical to Figure S7 except that data for the bromodomain of crebbp are shown.

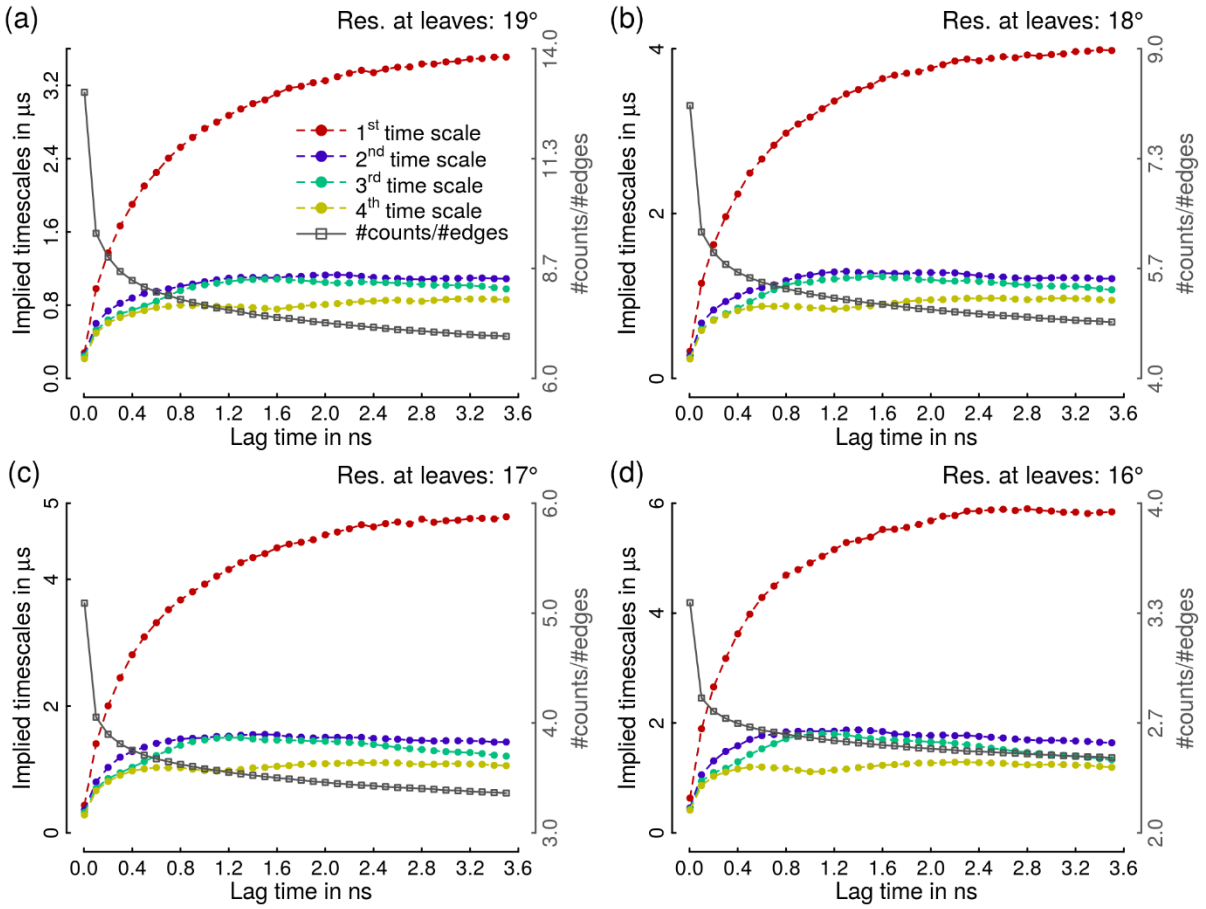

Figure S10. Implied time scales as a function of lag time and clustering resolution for baz2a. This figure is identical to Figure S7 except that data for the bromodomain of baz2a are shown.